

AperTO - Archivio Istituzionale Open Access dell'Università di Torino

## Physico-chemical characterization of playground sand dust, inhalable and bioaccessible fractions

### **This is the author's manuscript**

*Original Citation:*

*Availability:*

This version is available <http://hdl.handle.net/2318/1648916> since 2022-07-12T12:56:10Z

*Published version:*

DOI:10.1016/j.chemosphere.2017.09.101

*Terms of use:*

Open Access

Anyone can freely access the full text of works made available as "Open Access". Works made available under a Creative Commons license can be used according to the terms and conditions of said license. Use of all other works requires consent of the right holder (author or publisher) if not exempted from copyright protection by the applicable law.

(Article begins on next page)

1  
2  
3  
4  
5  
6 **This is the author's final version of the contribution published as:**  
7

Iris H.Valido, Elio Padoan, Teresa Moreno, Xavier Querol, Oriol Font, Fulvio Amato

Chemico-physical characterization of playground sand dust, inhalable and bioaccessible fractions

Chemosphere, Volume 190, January 2018, Pages 454-462

<https://doi.org/10.1016/j.chemosphere.2017.09.101>

8  
9  
10 **The publisher's version is available at:**

11  
12 <http://www.sciencedirect.com/science/article/pii/S0045653517315175>

13  
14  
15 **When citing, please refer to the published version.**

31 **Chemico-physical characterization of playground sand dust, inhalable and**  
32 **bioaccessible fractions**

33  
34 **Iris H. Valido<sup>a,\*</sup>, Elio Padoan<sup>a,b</sup>, Teresa Moreno<sup>a</sup>, Xavier Querol<sup>a</sup>, Oriol Font<sup>a</sup>, Fulvio Amato<sup>a</sup>**

35  
36 <sup>a</sup> Institute of Environmental Assessment and Water Research (IDÆA), Spanish National Research Council  
37 (CSIC), Barcelona, Spain

38 <sup>b</sup> Dipartimento di Scienze Agrarie, Forestali e Alimentari (DISAFA), Università degli Studi di Torino,  
39 Grugliasco (Torino), Italy

40 <sup>\*</sup>Present address: Centre Grup de Tècniques de Separació en Química (GTS), Departament de Química,  
41 Universitat Autònoma de Barcelona, Bellaterra, Spain

42 **Corresponding author:**

43 Iris H. Valido

44 Centre Grup de Tècniques de Separació en Química (GTS), Departament de Química, Universitat Autònoma  
45 de Barcelona, Edifici C, Av. De l'Eix Central, s/n, 08193 Cerdanyola del Vallès, Barcelona, Spain.

46 [iris.henriquez@uab.cat](mailto:iris.henriquez@uab.cat)

47  
48 **Abstract**

49 Dust is a mixture of natural and anthropogenic particles originated from multiple sources, which can  
50 represent an hazard for human health. Playgrounds are a site of particularly concern, due to sand dust  
51 ingestion by toddlers and inhalation. In this study, 37 sands used in public playgrounds in the city of  
52 Barcelona were physico-chemically characterized also in relation to routine maintenance activities such as  
53 disinfection and sand renewal. The analyzed sands show a felsic mineralogy dominated by Na-feldspar,  
54 quartz, and, to a lesser extent, K-feldspar, with minor amounts of clay minerals, carbonates and hematite.  
55 Particle fractions below 10, 2.5 and 1  $\mu\text{m}$  represent, on average, 0.65%, 0.17% and 0.07% of bulk volume,  
56 respectively, although, due to the human grinding, these initial fractions increased every year by a 18%, 5%  
57 and 2% respectively. Disinfection of sands effectively reduced only the  $\text{NH}_4^+$  concentration, among  
58 inorganic species. The average metal content was anthropogenically enriched, with respect to the upper  
59 continental crust, only for Sb and As. Both elements show high spatial variation indicating local sources such  
60 as road traffic for Sb (contributing mostly to the total concentration), and industry for As (also contributing  
61 with highly bioaccessible Sb, Cu and Zn). A clear inverse relationship between total concentrations of some  
62 elements and their leachable (Sb) and bioaccessible (Sb and Cr) fractions is observed. The most  
63 bioaccessible elements were  $\text{Ca} > \text{Ni} > \text{Cu} > \text{Sr} > \text{Cd} > \text{Pb}$ , all above the 25% of the total concentration.  
64 Bioaccessibility was higher for the carbonate-bearing particles and for the anthropic emitted metals (>50% of  
65 Ba, Cu, K, Pb and Zn).

67 **Keywords**

68 PMF; SBET extraction; metals; sand resuspension; PM10

69

70 **1. Introduction**

71

72 Dust is a mixture of natural and anthropogenic particles originated from multiple sources, which can  
73 represent a hazardous pollutant for human health via inhalation, ingestion, and, to a lesser extent, dermal  
74 contact (Paustenbach, 2000). A particularly sensible population is children, due to their higher inhalation rate  
75 and to the unintentional or deliberate ingestion of significant quantities of dust through hand-to-mouth  
76 contact (Ruby and Lowney, 2012; Acosta et al., 2009; Ljung et al., 2007; Banerjee, 2003; Calabrese et al.,  
77 1997). Incidental ingestion provides the primary pathway for human exposure; Shi et al. (2011) calculated  
78 that ingestion contributed 97.5% and 81.7% to the total exposure doses of non-carcinogenic and carcinogenic  
79 elements for children, and 91.7% and 52.9% for adults. The average amount of soil/sand dust ingested by a  
80 children has been calculated in various studies between 39 and 271 mg day<sup>-1</sup>, with a central estimate of 100  
81 mg day<sup>-1</sup>, representing the average dust intake for children within 1-6 years (USEPA, 2011). In addition,  
82 particle inhalation has been found to cause increased risk for respiratory and cardio-vascular disease and to  
83 affect the neurodevelopment of children (Sunyer et al., 2015). In urban environment, children exposure to  
84 dust occurs mostly during playground activities, as most of playgrounds are unpaved and sand particles are  
85 continuously ground by playing activities.

86 Particle size distribution is relevant for inhalation and ingestion processes. Inhalation involves mostly  
87 particles below hundreds of microns, although 10 microns (thoracic fraction) is the most common cut-off  
88 size for defining hazardous atmospheric particulate matter (PM). Incidental ingestion requires soil particles  
89 that can adhere to human hands, being finer particles (generally <63 µm in diameter) the more efficient in  
90 this behavior (Choate et al., 2006; Ruby and Lowney, 2012; Yamamoto et al., 2006).

91 As stated by the last report of air quality in Europe (EEA, 2015), PM limit values are often exceeded in  
92 Europe, mostly due to road traffic, industrial and biomass burning emissions. In addition, power generation,  
93 soil dust and shipping are also significant sources of PM. In the Barcelona Metropolitan Area the PM10 daily  
94 limit value was exceeded until 2013, due to the high concentrations observed at specific sites such as the  
95 Sants (in 2012) and El Prat de Llobregat (in 2013) monitoring sites. In both stations, the exceedances were  
96 mainly due to the high concentrations of the mineral component of PM, namely mineral dust, which consists  
97 of primary particles, generally coarser than 1 µm, and composed mainly by Al, Si, Ca, Fe, K and Ti, among  
98 other typical crustal species. Mineral dust can be emitted by multiple sources, including local soil  
99 resuspension, African dust outbreaks, construction works, and traffic-induced resuspension. Soil  
100 resuspension can increase considerably PM<sub>10</sub> levels also in school environment with sandy playgrounds  
101 (Amato et al., 2014).

102 Concerning the ingestion pathway, only a part of the ingested particles can be adsorbed and reach the  
103 systemic circulation (i.e. the bioavailable fraction), and the oral bioaccessibility is defined as the fraction that

104 is soluble in the gastrointestinal environment and available for absorption (Ruby et al., 1999). Therefore, *in*  
105 *vitro* tests of bioaccessibility are useful tools to predict the relative bioavailability, improving the accuracy of  
106 risk assessments in a cost-effective manner. In last years, bioaccessibility tests for soils have been developed  
107 and validated through comparison to the results of *in vivo* tests for specific metals (Oomen et al., 2002; Zia et  
108 al., 2011).

109 In this study we investigated the physico-chemical properties of sand dust in 37 public playgrounds in the  
110 city of Barcelona in relation to the risk for inhalation and ingestion for children, with the aim of: i)  
111 understanding the impact of sand use (two years period) on particle size distribution and metal contents; ii)  
112 understanding the impact of the regular maintenance activities (sand replacement and disinfection); iii)  
113 quantify the oral bioaccessibility of metals and their main sources.

114

## 115 **2. Methodology**

116

### 117 *2.1. Sampling and analytical treatment*

118 Thirty-seven parks within the city of Barcelona (NE, Spain) were selected and sampled on 11-12 December  
119 2014 based on (see Table SM1, in Supplementary Material) the:

120

121 • Time past from the last sand replacement (samples labelled as 01R to 12R). Replacement is performed  
122 with a 2-years frequency by the City Council. This selection allowed evaluating the impact of sand  
123 aging/grinding from December 2012 to October 2014. In order to minimize possible confounders due  
124 to disinfection and spatial variability, the selected playgrounds of this first batch were disinfected  
125 nearly at the same time and were located within the same district.

126 • Time past from the last disinfection (consisting in a cleaning of the top 10 cm layer with water at  
127 90°C) (samples labelled as 01D to 08D). Disinfection is performed with 2-months frequency by the  
128 City Council. The selected playgrounds were disinfected from 6<sup>th</sup> October to 29<sup>th</sup> November 2014 and,  
129 in order to minimize possible confounders due to renewal and spatial variability, the selected parks of  
130 this second batch had similar time past from the last renewal and were located as close as possible.  
131 Spatial distribution of metals in playgrounds in the area of Barcelona (includes samples labelled as  
132 01E to 13E and 01C to 05 C). The selected playgrounds sands of this batch were all replaced on  
133 February 2014, except for 01, 03, 04 and 05C, and were spread across the city.

134 • Location: Playgrounds located across the municipal terrain, with sand replaced at the same time  
135 (February 2014). Samples labelled as 01E to 13E.

136

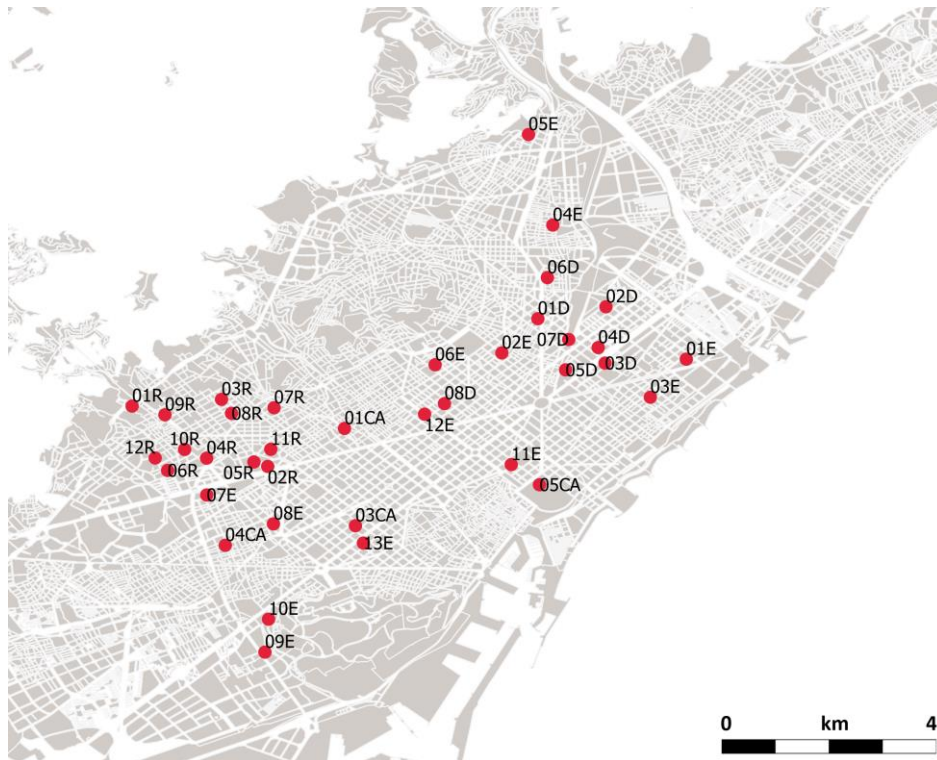


Figure 1. Map of playgrounds sampled across the city of Barcelona.

137

138

139

140 The sand sampling was performed within the top layer at 37 playgrounds using a PVC ring (5 cm height and  
 141 10 cm diameter), at two points of the playground (USEPA, 1992) not covered by the treetops, not at the edge  
 142 of the playground or near to vegetation or urban furniture and visibly dry. Each of the two subsamples  
 143 allowed the collection of 393 cm<sup>3</sup> of sand. In addition, one unexposed sand sample, not previously used for  
 144 other purposes (blank), was collected from the stock of the provider in charge of the sand replacement. Once  
 145 collected in a plastic bottle, samples were brought to the laboratory. Collected subsamples were mixed,  
 146 homogenized and quartered to the final mass needed for laboratory analysis (Fernández, 2006; VMGA,  
 147 2014). Sand humidity and porosity were calculated gravimetrically, after drying the samples during 24h in a  
 148 heater at 60°C and adding Milli-Q water until saturation (Asensio et al., 2012). For each sample, 200 g of  
 149 sand were then dried in plastic Petrie dishes in the stove at 60°C during 24h, and sieved at 63 µm by means  
 150 of a mechanic siever during 15 minutes.

151 Once sieved the (<63 µm) sample was divided into several fractions for different laboratory analyses:

- 152 • 5 g were leached in Milli-Q water for the determination of water soluble ions. To determine the  
 153 leaching potential of major and trace elements, we applied the European Standard leaching test EN-  
 154 12457 (according to Council decision 2003/33/EC), using a ratio liquid/solid (Milli Q water/sample)  
 155 of 10:1 under shaking for 24h. Then, the leachate was filtered using a syringe (BRAUN Injekt 10ml)  
 156 and a 0.45µm PVDF Whatman filter and the liquid part was analyzed: selective electrode for NH<sub>4</sub><sup>+</sup>,  
 157 High Performance Liquid Chromatography (HPLC Waters 1525) (for Cl<sup>-</sup>, NO<sub>3</sub><sup>-</sup>, and SO<sub>4</sub><sup>2-</sup>),  
 158 Inductively Coupled Plasma- Mass Spectrometry (ICP-MS, Thermo Fischer Scientific X-Series II), for  
 159 trace elements) and Atomic Emission Spectrometry (ICP-AES, Thermo Fischer Scientific iCAP 6500

160 Radial) for major elements. The samples sent to both ICPs were acidified to 2% HNO<sub>3</sub>. Besides that,  
161 the pH and ionic conductivity were determined by means of Thermo Scientific pHmeter and  
162 Ultrameter MyronL respectively.

- 163 • 150 mg were used for the grain size analysis, by means of a Malvern Mastersizer 2000 with Hydro  
164 2000G. The sample was dispersed in Milli Q water and analyzed between 0.01 and 2000 μm. From the  
165 spectrometric pattern acquired, the particle size distribution is calculated using the model of Mie's  
166 scattering theory.
- 167 • 1.5 g of each sample were milled for: 1 g for X-Ray Diffraction (XRD), 0.1 g for acid digestion and  
168 0.1 g to determine Total Carbon (TC) by means of an elemental LECO analyzer.

169

170 The powder XRD data were collected by a Bruker D8 A25 Advance X-ray diffractometer  $\theta$ - $\theta$ , with CuK $_{\alpha 1}$   
171 radiation, Bragg-Brentano geometry and a lineal LynxEyeXE detector. The XRD spectra were obtained from  
172 4° to 60° of 2-Theta with a step pf 0.015° and a counting time of 0.1s and the sample rotation. The  
173 quantitative analyses on 9 samples were instead performed from 4° to 120° of 2-Theta with a step of 0.015°  
174 and a counting time of 0.5s and the sample in rotation. The crystalline phase identification was carried out by  
175 standard Joint Committee on Powder Diffraction Standards (JCPDS) file by the computer program "EVA"  
176 (Bruker).

177 For elemental composition, the samples (<63μm) were acid-digested adapting a protocol used for PM  
178 samples (Querol et al., 2001), using 5 ml HF, 2.5 ml HNO<sub>3</sub> and 2.5 ml HClO<sub>4</sub>. For quality assurance,  
179 reference materials were also digested to determine the accuracy of the analytical and digestion methods:  
180 SRM 1633b (Trace Elements in Coal Fly Ash) and CANMET SO-2 and SO-4.

181 A widely used and tested method was used to assess the oral bioaccessibility: the Simple Bioaccessibility  
182 Extraction Method (SBET), consisting in an extraction with glycine at a buffered pH miming the conditions  
183 on the gastrointestinal tract of children (Drexler and Brattin, 2007; Oomen et al., 2002). Oral bioaccessible  
184 (SBET method) contents were determined mixing 0.25 g with 25 ml of extractant, a glycine 0.4 M solution  
185 with pH adjusted to 1.5 with concentrated HCl. Samples have been horizontally shaken at 37°C and 140 rpm  
186 for 1 h (Ruby et al., 1999; U.S. EPA, 2013). The mixture was then centrifuged at 3000 rpm for 10 min and  
187 the supernatant filtered through 0.45μm PVDF (Whatman) filters prior to analysis. The extract was analyzed  
188 for trace and major elements as above descript, except for P, S, As and V, not analyzed as the first two were  
189 present as impurities in the extracting solution and the last were highly interfered from the chloride.

190

### 191 *2.3 Source apportionment of metals*

192 Source apportionment techniques are used to apportion pollutants mass contributions to different  
193 source/factors which are able to explain most of the variance of observed pollutants concentrations. Source  
194 apportionment studies are generally performed by receptor models that are based on the mass conservation  
195 principle:

$$x_{ij} = \sum_{k=1}^p g_{ik} f_{jk} + e_{ij} \quad (1)$$

196

197 Where  $x_{ij}$  is the  $i^{\text{th}}$  concentration of the species  $j$ ,  $g_{ik}$  is the  $i^{\text{th}}$  contribution of the source  $k$  and  $f_{jk}$  is the  
 198 concentration of the species  $j$  in source  $k$ , while  $e_{ij}$  are the residuals. Equation (1) can be also expressed in  
 199 matrix form as  $\mathbf{X}=\mathbf{GF}^T$ . If  $f_{jk}$  are known for all the sources then the Chemical Mass Balance (CMB) can be  
 200 applied (Watson et al., 1984). For this model the experimental profiles of all major sources are needed. When  
 201 both  $g_{ik}$  and  $f_{jk}$  are unknown, factor analysis (FA) techniques such as *Principal Components Analysis* (PCA)  
 202 (Henry and Hidy, 1979; Thurston and Spengler, 1985) and *Positive Matrix Factorization* (PMF) (Paatero and  
 203 Tapper, 1994) are used for solving (1).

204 PMF solves equation (1) minimizing the object function  $Q$ :

$$Q = \sum_{i=1}^n \sum_{j=1}^m (e_{ij} / s_{ij})^2 \quad (2)$$

205

206 where  $s_{ij}$  are the individual data uncertainties. For all elements with concentrations above the detection limit  
 207 the uncertainty was expressed as 10% of the element concentration plus one third of the detection limit. For  
 208 elements with concentration below or equal to the detection limit, uncertainty was expressed as 0.83 times  
 209 the detection limit. The PMF was applied using US EPA's PMF software, Version 5.0 (Norris et al., 2014).  
 210 A total (dependent) variable was set as a constant value ( $10^6$  mg/kg) for all samples. The input data matrix  
 211 contained the 33 most significant elements/components concentrations, based on their signal-to-noise ratio  
 212 (Paatero and Hopke, 2003), the percentage of data above the detection limit and importance in tracing  
 213 specific sources. The distribution of residuals, G-space plots, Fpeak values and  $Q$  values were explored for  
 214 solutions with number of factors varying between 3 and 7.

215 The PMF method was also applied to the bioaccessible fraction of metals ( $\mu\text{g/g}$ ) as independent variables,  
 216 setting the sum of analyzed species as total variable. The input data contained the 18 most significant  
 217 analyzed elements (excluding ions, As, P, S and V due to the extraction matrix and Ce, La, Li, Mo, Rb, Se,  
 218 Sn, Ti and Zr, with high percentage of values below detection limit).

219

## 220 3. Results

221

### 222 3.1 Physico-chemical characteristics

223 The chemical characterization of sand samples (fraction below 63  $\mu\text{m}$ ) of playgrounds in the city of  
 224 Barcelona is reported in Table 1, and shows a main aluminum-silicate composition ( $\text{Al}_2\text{O}_3$  represents within  
 225 5.2-17.9 % of mass) followed by Ca-Mg carbonates ( $\text{CaO}+\text{MgO}$  sums within 0.5-10.1 % of mass).  
 226 Significant fractions of mass consist also of total carbon (TC),  $\text{Fe}_2\text{O}_3$ ,  $\text{K}_2\text{O}$ ,  $\text{Na}_2\text{O}$  and  $\text{P}_2\text{O}_5$  ( $1.1\pm 0.9\%$ ,  
 227  $4.0\pm 0.9\%$ ,  $5.2\pm 1.1\%$ ,  $4.0\pm 1.0\%$ ,  $0.21\pm 0.15\%$ , respectively). The sum of  $\text{SO}_4^{2-}$ ,  $\text{NO}_3^-$ ,  $\text{NH}_4^+$  and  $\text{Cl}^-$  represents  
 228 only 0.003-0.3% of the mass, while trace elements sum 0.2-1.0% of the mass. The most abundant trace



229 elements are Ti, Mn, Ba, Zr, Zn, Rb, and Sr, with mean concentrations of 3130, 894, 562, 369, 166, 158, and  
 230 80 µg/g, respectively.

231

232 Table 1. Total concentrations (µg/g), bioaccessible fraction (%) and leachable fraction (%) of the  
 233 analyzed metals. na: not analyzed

Element	Mean Total concentration (µg/g)	Mean bioaccessible fraction (%)	Mean leachable fraction (%)	Element	Mean Total concentration (µg/g)	Mean bioaccessible fraction (%)	Mean leachable fraction (%)
<b>Al</b>	75571	1	<0.1	<b>Ni</b>	9.3	44	<0.1
<b>As</b>	12	na	0.2	<b>P</b>	0.05	na	1
<b>Ba</b>	561	8	<0.1	<b>Pb</b>	62	27	<0.1
<b>Ca</b>	15954	64	2	<b>Rb</b>	158	<1	<0.1
<b>Cd</b>	0.97	30	0.2	<b>S</b>	93	na	7
<b>Co</b>	3.7	21	0.1	<b>Sb</b>	2.2	14	3
<b>Cr</b>	19	20	<0.1	<b>Se</b>	1.1	41	0.3
<b>Cu</b>	26	36	0.2	<b>Sn</b>	18	< 0.1	<0.1
<b>Fe</b>	27852	1	<0.1	<b>Sr</b>	81	28	1
<b>K</b>	37670	1	<0.1	<b>Ti</b>	3147	0.5	<0.1
<b>La</b>	57	8	<0.1	<b>U</b>	10	4	<0.1
<b>Li</b>	27	2	0.4	<b>V</b>	40	na	<0.1
<b>Mg</b>	4496	17	0.6	<b>W</b>	14	22	2
<b>Mn</b>	887	24	0.1	<b>Zn</b>	166	16	<0.1
<b>Mo</b>	1.4	4	6	<b>Zr</b>	361	<0.1	<0.1
<b>Na</b>	26846	1	<0.1				

234

235 We calculated the Enrichment Factors (EFs) for all elements, normalizing the concentration of the element  
 236 with the concentration of Al in the average Earth upper-crust (Taylor and McLennan, 1995). Mean values for  
 237 samples are reported in Figure SM1, in the Supplementary Material, together with values for the unexposed  
 238 sand sample (blank). The majority of the elements appear not to be significantly enriched in sands, averaging  
 239 all samples, while only As, Cd and Sb showed EFs around 10 (9, 10 and 12, respectively). With respect to  
 240 the unexposed sample, however, only As and Sb showed enrichment, which is noteworthy considering the  
 241 little time of exposure of sand to the atmospheric metals deposition.

242 The sand particle grain size (% in volume) shows a typically coarse size distribution (Figure SM2) being the  
 243 inhalable fraction (below 63 µm) 3.72% on average. The presence of clay minerals and mica is likely  
 244 responsible for the significant fraction of particles below 2 µm. The thoracic fraction (<10 µm) accounted  
 245 typically for 0.65% of bulk volume (or mass, assuming constant particle density), while the fraction below  
 246 2.5 and 1 µm are in average 0.17% and 0.07%, respectively.

### 247 3.2 Mineralogy

248 The XRD results (Table SM2) show a felsic mineralogy dominated by Na-feldspar, quartz, and, to a lesser  
249 extent, K-feldspar, with minor amounts of clay minerals (illite>chlorite), carbonates (mostly calcite) and  
250 traces of hematite.

251 According to the quantitative estimate of relative amounts on 9 samples (batch D: samples with same time of  
252 use and the unexposed sample), Na-feldspar is the most common mineral present (27-48%), followed by K-  
253 feldspar (13-23%) and quartz (9-23%). Illite and chlorite amounts range within 11-27% and 6-11%  
254 respectively. In addition, dolomite and calcite were also detected although not in all the samples and up to  
255 6% and 4% of total mass, while hematite was only in trace content.

256 The source for these feldspathic sandstones is likely to be mainly from weathered granites (possibly with  
257 some influence from metamorphic materials). Much of the illite could derive from altered muscovite mica,  
258 the chlorite and hematite from altered biotite mica, and the calcite from the minor amount of calcium present  
259 in Na-feldspar.

260 With regard to the geology surrounding Barcelona, there is more exposure of the Palaeozoic granitoid  
261 basement around the River Besos valley than the Llobregat (although there is granodiorite exposed at least as  
262 far SW as the hill of Sant Pere Martir, and this may have fed granitic material into the Llobregat at least  
263 since Plio-Pleistocene times). The thick Pleistocene sediments flanking the Collserola hills generally contain  
264 much weathered granitic detritus. The abundance of feldspar makes these sandstones sedimentologically  
265 immature, so it is likely that they are sourced from mostly local materials deposited fluviially.

266 The mineralogy affects particle size distribution as when the percentage of quartz increases, the fraction (in  
267 volume) of soil particles below 10 microns decreases ( $R^2=0.56$ ), due to the coarser size distribution of quartz  
268 particles (the same was expected for the fractions below 2.5 and 1 microns, but the trend was not so clear).  
269 The potential impact on emissions due to resuspension is therefore lower for quartz-rich sands, rather than  
270 for typical fluvial sands, enriched in feldspars and fine clay minerals.

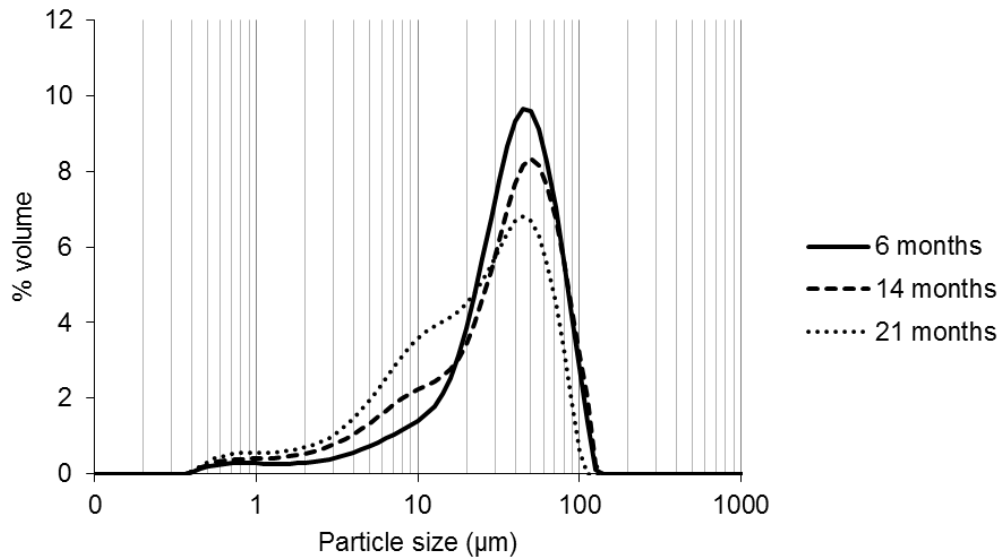
271

### 272 *3.3 Effects of maintenance activities*

273 One of the main goals of the study was to evaluate the impact of sand use (i.e. time past from the last sand  
274 replacement) on the physico-chemical characteristics. Regarding the particle size distribution, it can be  
275 observed a general increasing proportion of respirable fractions with the time of use (Figure SM3). Sands  
276 become therefore finer over time, by an average rate of 17.7%, 4.7% and 2.0%, for the fractions <10  $\mu\text{m}$ ,  
277 <2.5  $\mu\text{m}$  and <1  $\mu\text{m}$  respectively, per year.

278 Figure 2 shows the full size distribution of particle volume for three samples collected after 6, 14 and 21  
279 months of use, respectively. It can be clearly observed the increase in fraction below 20  $\mu\text{m}$  (from the  
280 “youngest” (less used sand: 20%) to the “oldest” sample (more used sand: 49%)) in terms of their use in  
281 public playgrounds.

282



283  
 284 Figure 2. Size distribution of particle volume in sand samples collected after 6, 14 and 21 months of  
 285 use.

286 Concerning the metal content, results show no clear impact of time of use on the buildup of metals, probably  
 287 due to the relatively little time of exposure (<2 years). Unexpectedly, some metals such as Cr, Ni and Pb  
 288 show higher concentrations in sands newly replaced, suggesting a relevant contribution from bedrock  
 289 materials such as carbonates (Cr and Ni, see section 3.5) and feldspars (Pb, see section 3.5). Similarly,  
 290 neither TC nor soluble compounds showed higher concentrations in the “oldest” samples.

291 Regarding the treatment of disinfection that is carried out every 2 months in the playgrounds, it can be  
 292 observed that the effect on the inorganic fraction of sand is limited to a decreasing trend on the concentration  
 293 of  $\text{NH}_4^+$  (Figure SM4). The  $\text{NH}_4^+$  concentration seems to increase exponentially with time after the last  
 294 disinfection ( $R^2=0.58$ ), probably due to the atmospheric deposition of ammonium salts. No clear effect on  
 295 other soluble components, such as  $\text{SO}_4^{2-}$ ,  $\text{NO}_3^-$  or  $\text{Cl}^-$  was found. Neither metals seem to have been affected  
 296 by this treatment, due to their low solubility in water (<6%). No effect on particle size distribution was  
 297 found.

### 298 3.4 Spatial variability

299 Enrichment factors were explored in the spatial domain of the city. Cadmium, as shown earlier, was enriched  
 300 by a factor of 9 with respect to the Earth crust, but not enriched with respect to the local unexposed sand. The  
 301 range of enrichment variability was low across the city (Figure 3), showing a maximum EF of 1.6 (with  
 302 respect to the unexposed sand). Conversely As showed a clearer spatial pattern in the anthropogenic  
 303 signature across the city, displaying maxima enrichments towards the coastal part of the city, although no  
 304 clear association to specific sources can be drawn. Antimony, mainly emitted from non-exhaust sources  
 305 (Schauer et al., 2006), showed also little variation across the city, however no correlation was found between  
 306 metals concentrations and time of exposure or traffic density.  
 307

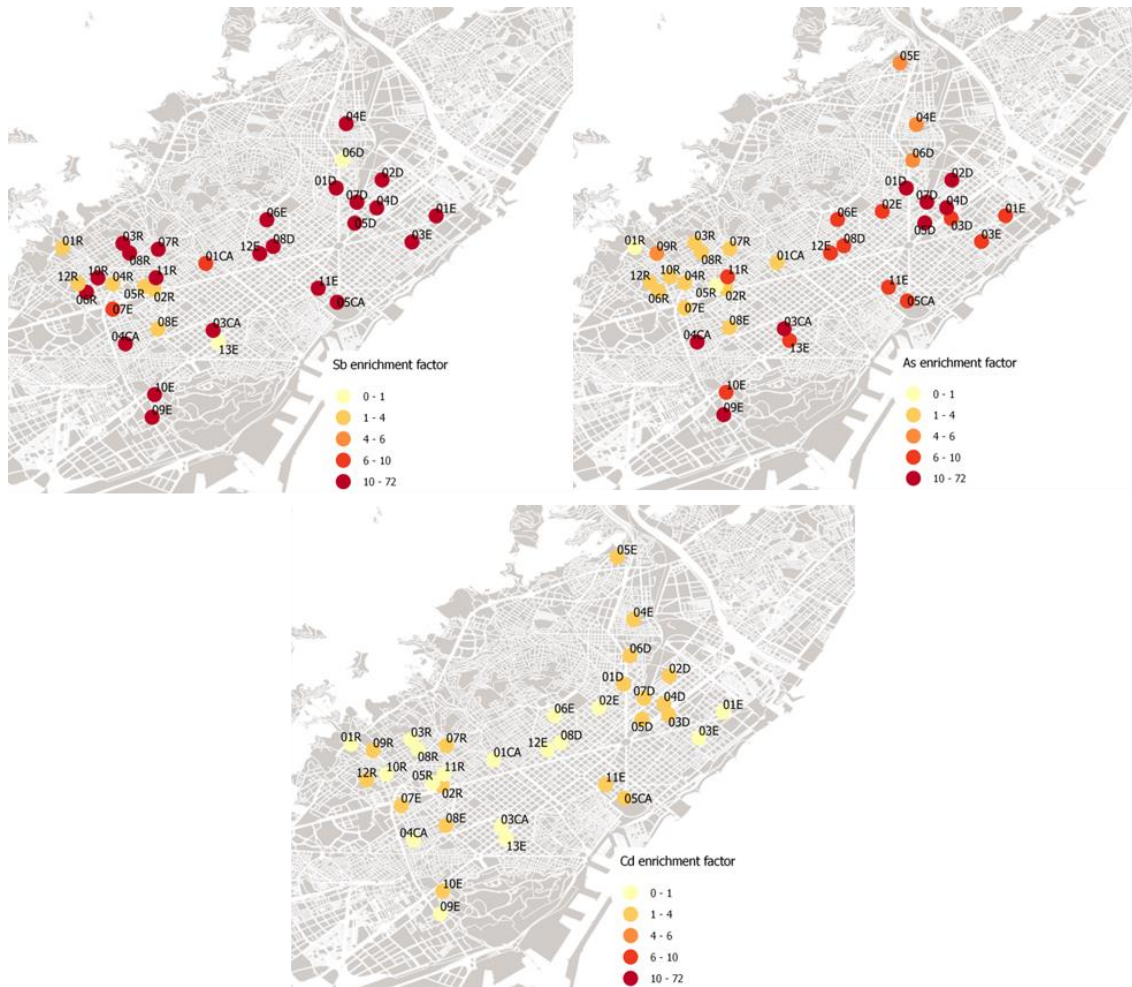


Figure 3. Maps of Enrichment factors calculated for Sb, As and Cd with respect to the unexposed sand.

308

309

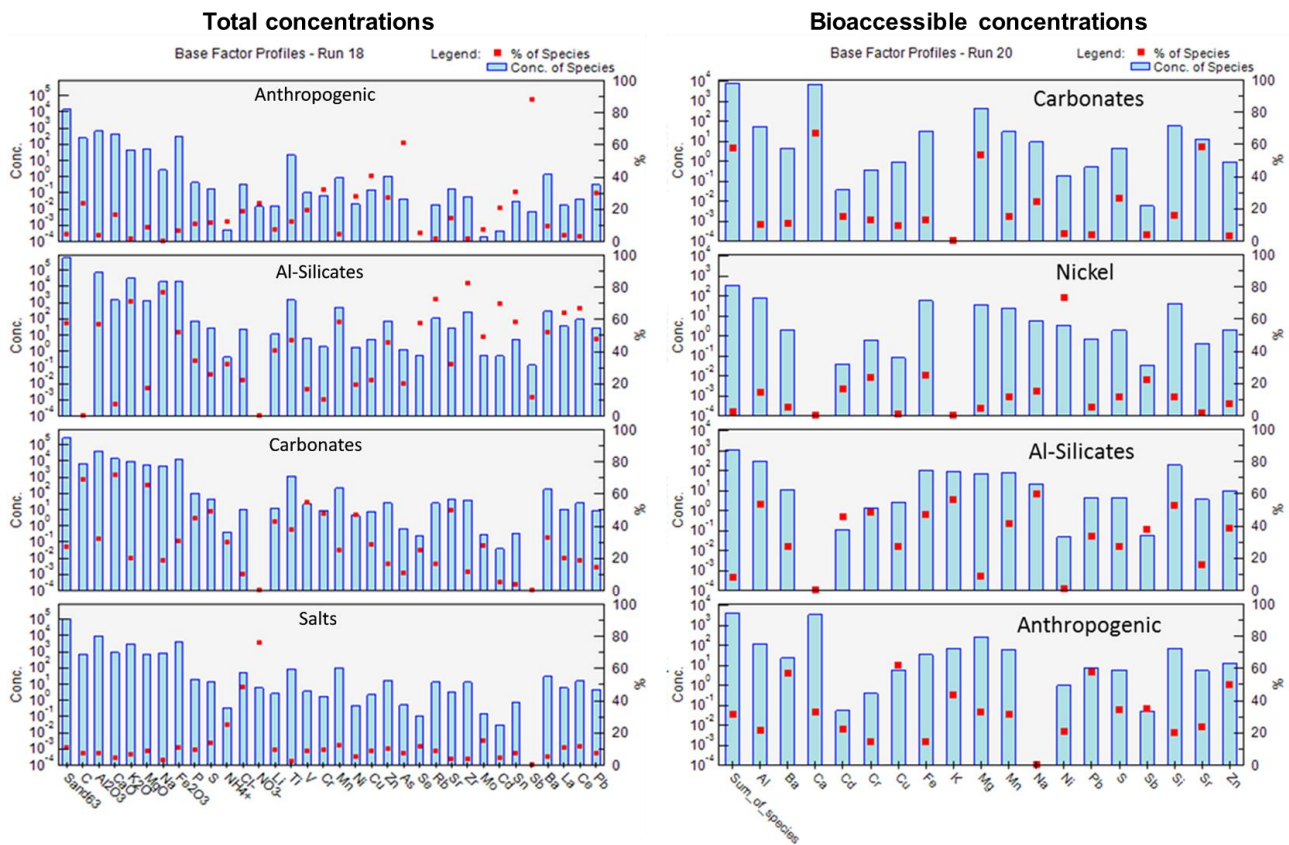
310

311 Spatial Distribution analysis revealed also higher levels of  $\text{NO}_3^-$  and  $\text{NH}_4^+$  in parks located in the NE part of  
 312 the city (Figure SM5), next to a methane-fueled power plant, although this part of the city, which is at the  
 313 lowest altitude and a shallow top layer of the phreatic zone, can be also influenced by leaking from sewage  
 314 system.

315

### 316 3.5 Source apportionment of metals

317 The PMF solution for total metal concentrations ( $<63 \mu\text{m}$ ) revealed four factors/sources, namely  
 318 Anthropogenic, Al-Silicates, Salts and Carbonates (Figure 4). These sources contributed, in average, 4.3%,  
 319 57.6%, 10.6% and 27.5% to the sand material below  $63 \mu\text{m}$ .



320

321

Figure 4. PMF factor profiles for total (left) and bioaccessible (right) concentrations. Blue bars indicate average absolute species concentration (mg/kg, left axis), red dots indicate % of specie due to each source.

322

323

324

The Anthropogenic source was identified from the high share of Sb, As, Cu explained by this source. Sb and Cu are commonly used as brake wear tracers (Schauer et al., 2006), but can also be emitted by metallurgical industry (Amato et al., 2009), as for As. The chemical profile of this factor is dominated by  $\text{Fe}_2\text{O}_3$ , C, S,  $\text{Al}_2\text{O}_3$  and CaO. It is also noteworthy the significant share of Sn, Cr, Pb and Mn explained by this source.

328

The Al-Silicates source is the main responsible for the total composition, explaining most of the variation of  $\text{Al}_2\text{O}_3$ , NaO,  $\text{K}_2\text{O}$ ,  $\text{Fe}_2\text{O}_3$ , Rb, Ti and Mn, which are related to clay minerals (illite, and chlorite) and feldspars (microcline and albite). This factor also shows the majority of Zr, Sn and Pb, which all have affinity to aluminum silicates.

332

The third factor, labelled as Salts, explained most of  $\text{Cl}^-$  and  $\text{NO}_3^-$  variation, and (to a lesser extent)  $\text{NH}_4^+$ , suggesting the presence of ammonium salts and sea salt from atmospheric deposition.

334

The fourth factor is clearly related to carbonates, showing high loading of CaO, MgO, C, but also Sr, Ba and Ni, which are quite common in calcite and dolomite. The presence of S and Ba may indicate also the presence of barite.

337

According to PMF results, more than 50% of S, Cu, Sb, and As in sands are originated from anthropogenic sources, although only As and Sb show high enrichment factors with respect to the average composition of Earth crust and the unexposed sand.

339

340 In spite of the clear anthropogenic contribution (related, probably, mainly to traffic and industry), no  
341 correlation was found between the anthropogenic factor and the traffic density (vehicles m<sup>-2</sup>, data provided  
342 from the Catalan Government, Table SM1), suggesting that the most relevant traffic contribution is from  
343 background rather than from street-level emissions.

344

### 345 *3.6 Leachable and bioaccessible fractions*

346 The pH of the leachates of the playground sands are slightly alkaline, with values ranging from 7.1 to 7.9.  
347 Mean leachable fraction of each element is listed in Table 1. The most soluble elements were S, Mo, Sb, Ca,  
348 and Sr, although their soluble fraction does not exceed 7%, 6%, 3%, 2% and 1%, respectively. Therefore, the  
349 solubility is not related to specific sources, as S and Mo are mostly explained from the Al-Silicates factor, Sb  
350 from the Anthropogenic and Ca and Sr from the Carbonates factor.

351 In several elements (i.e. Sb, Ca, Cd, Zn, Cr, Zr, Ni, Sr and Mg) it has been observed that the higher the total  
352 concentration of the element (µg/g), the lower the leachable fraction (%), which might suggest a different  
353 speciation and solubility of the metals emitted by the different sources. Antimony, for example, (see Figure  
354 SM6, in Supplementary Material) was found to be mostly anthropogenic (as shown by PMF results),  
355 showing a higher solubility at lower concentrations, especially in the SW part of the city, which suggests a  
356 more industrial (with high temperature process and finer size distribution) origin of the bioaccessible  
357 fraction.

358 Bioaccessibility extraction test is used to determine the metal fraction that would dissolve in the gastric  
359 environment and become available for absorption. Results for all analyzed elements are reported in Table 1  
360 as percentage of the total content.

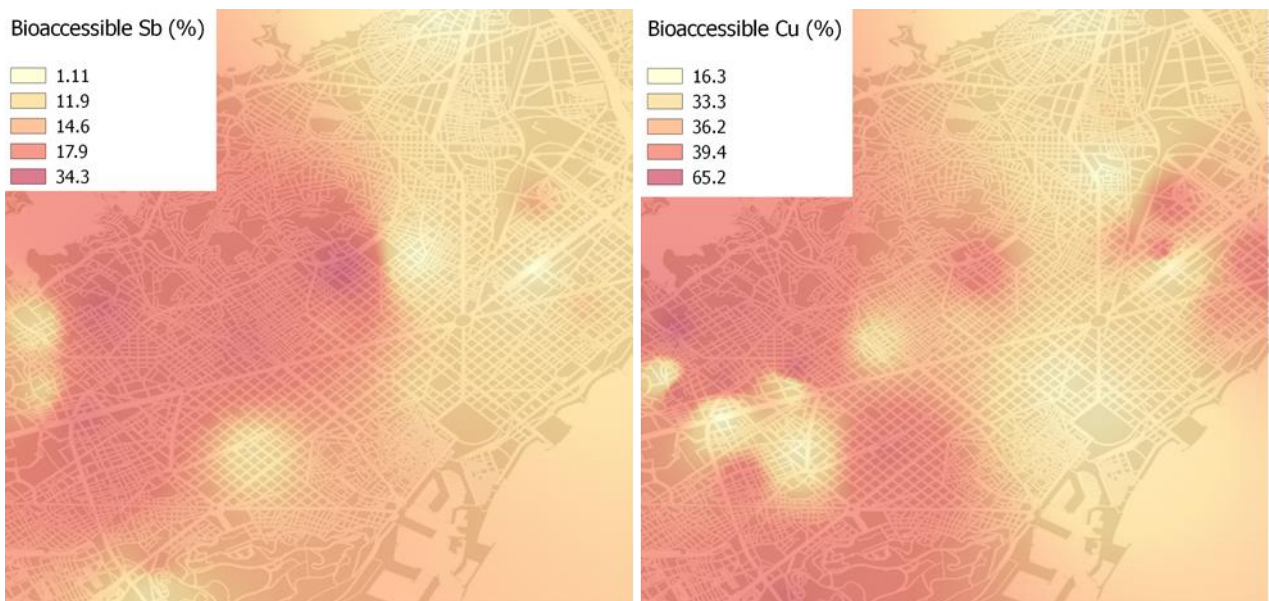
361 Average values of bioaccessibility varies from 0.002% of Zr to 64% of Ca, but some of the most harmful  
362 metals, such as Ni, Cu, Cd, Pb and Sb, were also among the most bioaccessible (from 14% to 41%),  
363 including Se.

364 The leachable fraction of Sb and Cr showed lower bioaccessible percentages in samples with higher  
365 concentrations (Figure SM7). As for total concentration, the relationship between the bioaccessible fraction  
366 with disinfection and time of use was explored but no significant relationships were seen.

367 Spatial distribution of the bioaccessible contents was explored across the city. Cadmium, which showed the  
368 higher variability range for bioaccessibility, did not show a clear spatial pattern, coherently with the  
369 relatively low anthropogenic contribution. Antimony showed a higher bioaccessibility in the SW region of  
370 the city (Figure 5), although this does not exceed 35%, where also the lowest concentrations were found.  
371 Therefore road traffic, responsible for most (80%) of the Sb, produces probably less bioaccessible Sb than  
372 industrial processes. This is in agreement with studies indicating that natural and mechanical wear  
373 contribution is less bioaccessible than high temperature emission processes (Ljung et al., 2007; Madrid et al.,  
374 2008; Wang et al., 2015). In fact, no relationship was found between traffic density and bioaccessible  
375 relative (or absolute) concentrations of metals. Similarly to Sb, higher bioaccessibility in the SW of the city  
376 was found for Cu and Zn, which are emitted from both traffic and industrial combustion sources (Amato et



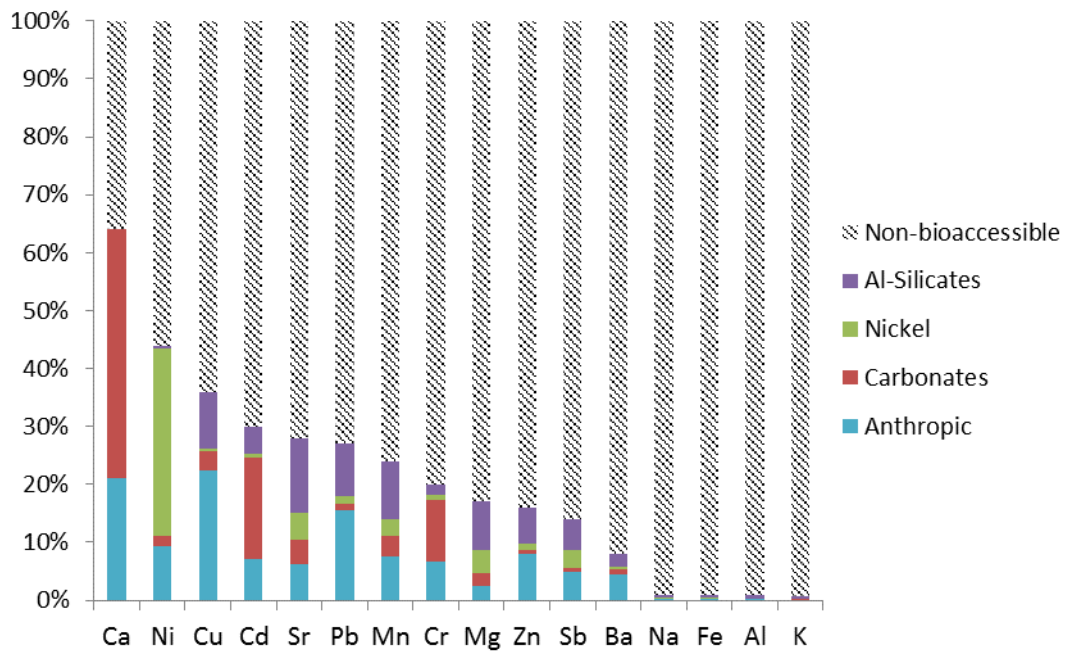
377 al., 2009; Minguillón et al., 2012) but a higher bioaccessibility for the industrial emitted particles can be  
378 deduced (Wang et al., 2015).  
379



380  
381 Figure 5. Spatial interpolation of the bioaccessible fraction (%) of Sb and Cu across the city of  
382 Barcelona.  
383

384 The PMF analysis applied to the bioaccessible metal concentrations (Figure 4) revealed four factors,  
385 similarly to the solution found for the total metal concentration. The similar sources identified were  
386 Carbonates, Anthropogenic and Al-Silicates, while and a Nickel factor (contributing very little to the sum of  
387 species) was found instead of the Salts factor. Relative contribution to the sum of bioaccessible species was,  
388 on average, 58%, 32%, 8% and 2%, respectively. Unfortunately, no separation of the Anthropogenic factor  
389 could be achieved. These results are coherent with the first PMF if we consider that the Salts factor could not  
390 be resolved, as in the SBET extract ions were not analyzed. Factor profiles are reported in Figure 4, while in  
391 Figure 6 the contribution of each factor to the total concentration.

392



393

394

Figure 6. Share of bioaccessible metals explained from each factor, as fraction of the total concentration.

395

396

397

398

399

400

401

402

403

404

405

406

407

408

409

410

411

412

413

414

According to PMF results, bioaccessible Sr, Mg, Cd and Ca are mainly explained by the Carbonates factors and, as expected, are among the most available; as carbonates dissolve at gastric pH, while elements explained mostly from the Al-Silicates factor are the least bioavailable, in average. More in detail, after Ca, the most bioaccessible metal is Ni, associated mostly to the Nickel factor and to the Anthropogenic, and this value is higher than what found in literature (Ljung et al., 2007; Padoan et al., 2016). Elements mainly explained by the Anthropogenic factor, as Cu and Sb, have a bioaccessible fraction of 36% and 14%, respectively, and also some Al-Silicates bearing metals, like Cd, Pb and Zn, have significant bioaccessible fraction. The mass of the Anthropogenic factor is dominated by Ca, Mg and Al, and it explains most of the variation of Ba, Cu, K, Pb and Zn.

Comparing PMF results for bioaccessible and total metal concentrations, the variation of metals explained by the different factors is generally similar except for Ba and K, whose bioaccessible fraction derives more from the Anthropogenic factor rather than geogenic (as for the total concentration), indicating that the anthropic input for these metals is more bioaccessible than the natural one, which dominates the total concentration, and Cr, shifting from the Carbonates to Al-silicates factor. Also Cu and Zn have a clearer anthropic signature in the bioaccessible fraction, rather than the total concentration, which helps identifying spatial patterns (see Figure 5 for Cu). The Ni-factor also shows significant contributions of Fe and Cr, pointing to steel particles. However, the identification of this factor is not definitively clear.



#### 415 **4. Conclusions**

416 Thirty-seven sands used in public playgrounds in the city of Barcelona were physico-chemically  
417 characterized in order to improve our understanding of their potential impact on risks due to dust ingestion  
418 by toddlers and inhalation. Routine maintenance activities were controlled, such as disinfection and sand  
419 replacement. The analyzed sands show a felsic mineralogy dominated by Na-feldspar, quartz, and, to a lesser  
420 extent, K-feldspar, with minor amounts of clay minerals (illite > chlorite), carbonates (mostly calcite) and  
421 traces of hematite. The particle size analysis shows a typically coarse distribution, although clay minerals are  
422 responsible for the significant fraction of particles below 2.5 µm. The fractions below 10, 2.5 and 1 µm  
423 represent, on average, 0.65%, 0.17% and 0.07% of the bulk volume, respectively, although due to the human  
424 grinding through playing, these initial fractions increase every year by a 18%, 5% and 2% respectively,  
425 confirming the environmental concern for air quality due to dust resuspension, which may cause local  
426 exceedances of PM<sub>10</sub> European limit standards. Bimonthly disinfection of sands was found to reduce  
427 significantly only the NH<sub>4</sub><sup>+</sup> concentration. The average metal content was anthropogenically enriched with  
428 respect to the upper continental crust, only for Sb (EF=12) and As (EF=10), while the enrichment of Cd  
429 (EF=9) may be linked to the local geology. Both Sb and As show high spatial variation, attributed to the  
430 anthropogenic source in PMF, although no clear separation can be done between industrial and road traffic  
431 contributions. The spatial distribution suggests background road traffic and industry as main sources of Sb  
432 (as no correlation was found with street level traffic density) and, less clearly, harbor and industry as main  
433 sources of As. A clear inverse relationship between total concentrations of some elements and their leachable  
434 (Sb) or bioaccessible (mostly Sb and Cr) fractions is observed. The most bioaccessible elements were  
435 Ca>Ni>Cu>Sr>Cd>Pb, all above the 25% of the total concentration. Bioaccessibility was higher for the  
436 carbonate-bearing particles and for the anthropic emitted metals, being more than 50% of the bioaccessible  
437 fraction of Ba, Cu, K, Pb and Zn originated from the anthropogenic source.

438

#### 439 **Acknowledgements**

440 The work was carried out in the framework of the Project “*Pruebas piloto para la mejora de la calidad del*  
441 *aire en colegios públicos*” funded by the Barcelona City Council.

442

#### 443 **Bibliography**

444 Acosta, J.A., Cano, A.F., Arocena, J.M., Debela, F., Martínez-Martínez, S., 2009. Distribution of metals in  
445 soil particle size fractions and its implication to risk assessment of playgrounds in Murcia City  
446 (Spain). *Geoderma* 149, 101–109. Doi:10.1016/j.geoderma.2008.11.034.

447 Amato, F., Pandolfi, M., Escrig, A., Querol, X., Alastuey, A., Pey, J., Perez, N., Hopke, P.K., 2009.  
448 Quantifying road dust resuspension in urban environment by Multilinear Engine: A comparison with  
449 PMF2. *Atmospheric Environment*, 43 (17), pp. 2770-2780. Doi: 10.1016/j.atmosenv.2009.02.039.

450 Amato, F., Rivas, I., Viana, M., Moreno, T., Bouso, L., Reche, C., Álvarez-Pedrerol, M., Alastuey, A.,  
451 Sunyer, J., Querol, X., 2014. Sources of indoor and outdoor PM<sub>2.5</sub> concentrations in primary  
452 schools. *Sci. Total Environ.* 490, 757–765. Doi:10.1016/j.scitotenv.2014.05.051.

453 Asensio, I., Moreno, S., Blanquer, H.G., Manuel, J., 2012. Técnicas de medida del espacio poroso del suelo.  
454 <http://hdl.handle.net/10251/16872>.

455 ASPB, Agencia de Salut Publica de Barcelona. Informe d'avaluació de la qualitat de l'aire a la ciutat de  
456 Barcelona Any 2012, 2013. [http://www.aspb.cat/quefem/docs/Qualitat\\_aire\\_2012.pdf](http://www.aspb.cat/quefem/docs/Qualitat_aire_2012.pdf).

457 Banerjee, A.D., 2003. Heavy metal levels and solid phase speciation in street dusts of Delhi, India. *Environ.*  
458 *Pollut.* 123, 95–105. Doi: 10.1016/S0269-7491(02)00337-8.

459 Calabrese, E.J., Stanek, E.J., James, R.C., Roberts, S.M., 1997. Soil ingestion: A concern for acute toxicity in  
460 children. *Environ. Health Perspect.* 105, 1354–1358.

461 Choate, L.M., Ranville, J.F., Bunge, A.L., Macalady, D.L., 2006. Dermally adhered soil: 1. Amount and  
462 particle-size distribution. *Integr. Environ. Assess. Manag.* 2, 375–384. Doi:  
463 10.1002/ieam.5630020409

464 Drexler, J.W., Brattin, W.J., 2007. An In Vitro Procedure for Estimation of Lead Relative Bioavailability:  
465 With Validation. *Hum. Ecol. Risk Assess. Int. J.* 13, 383–401. Doi:10.1080/10807030701226350

466 EEA, 2015. Air quality in Europe — 2015 report. European Environment Agency, EEA Report No 5/2015.

467 Fernández, L. et al., 2006. Manual de técnicas de análisis de suelos aplicadas a la remediación de sitios  
468 contaminados. Instituto Mexicano del Petróleo, Secretaría de Medio Ambiente y Recursos Naturales,  
469 Instituto Nacional de Ecología, México.

470 Henry, R.C., Hidy, G.M., 1979. Multivariate analysis of particulate sulfate and other air quality variables by  
471 principal components-Part I. *Atmospheric Environ.* 1967. Doi:10.1016/0004-6981(79)90068-4

472 Ljung, K., Oomen, A., Duits, M., Selinus, O., Berglund, M., 2007. Bioaccessibility of metals in urban  
473 playground soils. *J. Environ. Sci. Health Part A* 42, 1241–1250. Doi:10.1080/10934520701435684

474 Madrid, F., Biasioli, M., Ajmone-Marsan, F., 2008. Availability and bioaccessibility of metals in fine  
475 particles of some urban soils. *Arch. Environ. Contam. Toxicol.* 55, 21–32. Doi:10.1007/s00244-007-  
476 9086-1

477 Minguillón, M.C., Schembari, A., Triguero-Mas, M., de Nazelle, A., Dadvand, P., Figueras, F., Salvado,  
478 J.A., Grimalt, J.O., Nieuwenhuijsen, M., Querol, X., 2012. Source apportionment of indoor, outdoor  
479 and personal PM<sub>2.5</sub> exposure of pregnant women in Barcelona, Spain. *Atmospheric Environ.*, 59,  
480 pp. 426-436. Doi: 10.1016/j.atmosenv.2012.04.052

481 Norris, G., Duvall, R., Brown, S. and Bai, S., 2014. EPA Positive Matrix Factorization (PMF) 5.0  
482 Fundamentals and User Guide, EPA/600/R-14/108. Environ. Prot. Agency Off. Researc Dev.  
483 Publishing House Whashington DC 20460.

484 Oomen, A.G., Hack, A., Minekus, M., Zeijdner, E., Cornelis, C., Schoeters, G., Verstraete, W., Van de  
485 Wiele, T., Wragg, J., Rompelberg, C.J.M., Sips, A.J.A.M., Van Wijnen, J.H., 2002. Comparison of

486 Five In Vitro Digestion Models To Study the Bioaccessibility of Soil Contaminants. *Environ. Sci.*  
487 *Technol.* 36, 3326–3334. Doi:10.1021/es010204v

488 Paatero, P., Hopke, P.K., 2003. Discarding or downweighting high-noise variables in factor analytic models,  
489 in: *Analytica Chimica Acta*. pp. 277–289. Doi:10.1016/S0003-2670(02)01643-4

490 Paatero, P., Tapper, U., 1994. Positive Matrix Factorization - A Nonnegative Factor Model with Optimal  
491 Utilization of Error Estimates of Data Values. *Environmetrics* 5, 111–126.  
492 Doi:10.1002/env.3170050203

493 Padoan, E., Romè, C., Ajmone Marsan, F., 2016. Bioaccessibility and size distribution of metals in road dust  
494 and roadside soils along a peri-urban transect. *Sci. Total Environ.* 601-602, 89-98.  
495 Doi:10.1016/j.scitotenv.2017.05.180

496 Paustenbach, D.J., 2000. The practice of exposure assessment: a state-of-the art review. *J. Toxicol. Environ.*  
497 *Health Part B* 3, 179–291. Doi:10.1080/10937400050045264

498 Querol, X., Alastuey, A., Rodriguez, S., Plana, F., Mantilla, E., Ruiz, C.R., 2001. Monitoring of PM10 and  
499 PM2.5 around primary particulate anthropogenic emission sources. *Atmos. Environ.* 35, 845–858.  
500 Doi:10.1016/S1352-2310(00)00387-3

501 Ruby, M.V., Lowney, Y.W., 2012. Selective Soil Particle Adherence to Hands: Implications for  
502 Understanding Oral Exposure to Soil Contaminants. *Environ. Sci. Technol.* 46, 12759–12771.  
503 Doi:10.1021/es302473q

504 Ruby, M.V., Schoof, R., Brattin, W., Goldade, M., Post, G., Harnois, M., Mosby, D.E., Casteel, S.W., Berti,  
505 W., Carpenter, M., Edwards, D., Cragin, D., Chappell, W., 1999. Advances in Evaluating the Oral  
506 Bioavailability of Inorganics in Soil for Use in Human Health Risk Assessment. *Environ. Sci.*  
507 *Technol.* 33, 3697–3705. Doi:10.1021/es990479z

508 Schauer, J.J., Lough, G.C., Shafer, M.M., Christensen, W.F., Arndt, M.F., DeMinter, J.T., Park, J.-S., 2006.  
509 Characterization of metals emitted from motor vehicles. *Res. Rep. Health Eff. Inst.* 1-76-88.

510 Shi, G., Chen, Z., Bi, C., Wang, L., Teng, J., Li, Y., Xu, S., 2011. A comparative study of health risk of  
511 potentially toxic metals in urban and suburban road dust in the most populated city of China. *Atmos.*  
512 *Environ.* 45, 764–771. Doi:10.1016/j.atmosenv.2010.08.039

513 Sunyer, J., Esnaola, M., Alvarez-Pedrerol, M., Forns, J., Rivas, I., López-Vicente, M., Suades-González, E.,  
514 Foraster, M., Garcia-Esteban, R., Basagaña, X., others, 2015. Association between traffic-related air  
515 pollution in schools and cognitive development in primary school children: a prospective cohort  
516 study. *PLoS Med* 12, e1001792. Doi: 10.1371/journal.pmed.1001792

517 Taylor, S.R., McLennan, S.M., 1995. The geochemical evolution of the continental crust. *Rev. Geophys.* 33,  
518 241–265. Doi: 10.1029/95RG00262

519 Thurston, G.D., Spengler, J.D., 1985. A quantitative assessment of source contributions to inhalable  
520 particulate matter pollution in metropolitan Boston. *Atmospheric Environ. - Part Gen. Top.* 19, 9–25.  
521 Doi:10.1016/0004-6981(85)90132-5

522 U.S. EPA, 1992. Preparation of soil sampling protocols: Sampling techniques and strategies. U.S.  
523 Environmental Protection Agency, EPA/600/R-92/128.

524 U.S. EPA, 2011. Exposure Factors Handbook 2011 Edition (Final). U.S. Environmental Protection Agency,  
525 EPA/600/R-09/052F.

526 U.S. EPA, 2013. Method 1340, In vitro bioaccessibility assay for lead in soil. U.S. Environmental Protection  
527 Agency, SW-846 Update VI.

528 VMGA, 2014. Vice Ministerio de Gestión Ambiental, D.G. de C.A., 2014. Guía para muestreo de suelos.

529 Wang, Q., Ma, Y., Tan, J., Zheng, N., Duan, J., Sun, Y., He, K., Zhang, Y., 2015. Characteristics of size-  
530 fractionated atmospheric metals and water-soluble metals in two typical episodes in Beijing.  
531 Atmospheric Environ., 119, 294-303. Doi:10.1016/j.atmosenv.2015.08.061

532 Watson, J.G., Cooper, J.A., Huntzicker, J.J., 1984. The effective variance weighting for least squares  
533 calculations applied to the mass balance receptor model. Atmospheric Environ. - Part Gen. Top. 18,  
534 1347–1355. Doi:10.1016/0004-6981(84)90043-X

535 Yamamoto, N., Takahashi, Y., Yoshinaga, J., Tanaka, A., Shibata, Y., 2006. Size distributions of soil  
536 particles adhered to children's hands. Arch. Environ. Contam. Toxicol. 51, 157–163.  
537 Doi:10.1007/s00244-005-7012-y

538 Yu, B., Wang, Y., Zhou, Q., 2014. Human Health Risk Assessment Based on Toxicity Characteristic  
539 Leaching Procedure and Simple Bioaccessibility Extraction Test of Toxic Metals in Urban Street  
540 Dust of Tianjin, China. PLoS ONE 9, e92459. Doi:10.1371/journal.pone.0092459

541 Zia, M.H., Codling, E.E., Scheckel, K.G., Chaney R.L., 2011. In Vitro and in Vivo Approaches for the  
542 Measurement of Oral Bioavailability of Lead (Pb) in Contaminated Soils. Environmental Pollution  
543 159, 2320-2327. Doi:10.1016/j.envpol.2011.04.043